

One-Flavon Flavor: A Single *Hierarchical* Parameter B Organizes Quarks & Leptons at M_Z

Vernon Barger¹

¹Department of Physics, University of Wisconsin–Madison, Madison, WI 53706, USA

(Dated: December 16, 2025)

Flavor hierarchies emerge from a single hierarchical parameter B in a one-flavon Froggatt–Nielsen scheme. Fixing $B = 5.357$ from charged-lepton ratios ($m_e : m_\mu : m_\tau \propto \epsilon^5 : \epsilon^2 : 1$, $\epsilon = 1/B$), we reproduce quark masses and CKM targets at M_Z with $\mathcal{O}(1)$ coefficients. The same ϵ gives viable lepton textures and benchmarks for U_{PMNS} , $\sum m_\nu$, and $m_{\beta\beta}$. Compact correlations ($|V_{us}|, |V_{cb}|, |V_{ub}|, \theta_{13}^{\text{PMNS}}$) follow from powers of ϵ .

I. INTRODUCTION

The observed hierarchies of quark and lepton masses and mixings span many orders of magnitude, yet are accurately described by the Standard Model (SM) Yukawa sector with apparently arbitrary $\mathcal{O}(1)$ complex parameters. Froggatt–Nielsen (FN) models [1] offer a simple organizing principle: a spontaneously broken $U(1)_{\text{FN}}$ symmetry and one or more flavon fields generate hierarchical Yukawas via powers of a small parameter $\epsilon = \langle \phi \rangle / \Lambda$.

In this work we show that a *single* hierarchical parameter B —fixed by charged-lepton ratios—organizes the entire set of quark and lepton hierarchies at M_Z in a one-flavon FN scheme. Concretely, we take

$$B \equiv \frac{1}{\epsilon}, \quad m_e : m_\mu : m_\tau \propto \epsilon^5 : \epsilon^2 : 1, \quad (1)$$

and fit B from charged-lepton data.¹ With $B = 5.357$ ($\epsilon = 0.187$) we obtain simple integer FN exponents for the Yukawa textures and reproduce quark masses and the leading CKM/PMNS structures with near-unity complex coefficients.

We work with a minimal one-flavon $U(1)_{\text{FN}}$ framework and provide an explicit benchmark set of complex $\mathcal{O}(1)$ matrices that reproduces:

- quark masses at M_Z (Table II),
- CKM magnitudes and phase (Table III, Eqs. (34)–(35)),
- PMNS mixing angles and a benchmark leptonic Dirac phase (Eqs. (24), (37)),

for a fixed FN charge choice taken from the scan of Ref. [3]. We also show explicitly how the extracted $\mathcal{O}(1)$ coefficients behave in a Type-II 2HDM interpretation with $\tan\beta = 40$ and in the single-Higgs SM.

II. FN FRAMEWORK AND EXPONENTS

A. FN Lagrangian

We work with a Froggatt–Nielsen $U(1)_{\text{FN}}$ symmetry with one flavon ϕ of charge $q(\phi) = -1$, and a single Higgs doublet H with $q(H) = 0$. We define

$$\epsilon \equiv \frac{\langle \phi \rangle}{\Lambda} = \frac{1}{B}, \quad B = 5.357 \Rightarrow \epsilon \simeq 0.187, \quad (2)$$

so that Yukawa entries scale as integral powers of ϵ .

The FN expansion of the Yukawa and Weinberg operators is

$$\begin{aligned} \mathcal{L}_{\text{FN}} \supset & \sum_{ij} \lambda_{ij}^u \left(\frac{\phi}{\Lambda} \right)^{n_{ij}^u} \bar{Q}_i H u_j^c + \sum_{ij} \lambda_{ij}^d \left(\frac{\phi}{\Lambda} \right)^{n_{ij}^d} \bar{Q}_i \tilde{H} d_j^c \\ & + \sum_{ij} \lambda_{ij}^e \left(\frac{\phi}{\Lambda} \right)^{n_{ij}^e} \bar{L}_i \tilde{H} e_j^c \\ & + \frac{1}{\Lambda_L} \sum_{ij} \kappa_{ij} \left(\frac{\phi}{\Lambda} \right)^{n_{ij}^\nu} (\bar{L}_i \tilde{H})(\bar{L}_j \tilde{H}) + \text{h.c.} \end{aligned} \quad (3)$$

with $\tilde{H} = i\sigma_2 H^*$ and integer exponents n_{ij}^f determined by the $U(1)_{\text{FN}}$ charges. After electroweak symmetry breaking (EWSB) with $\langle H \rangle = v/\sqrt{2}$, the Higgs vev sets the overall mass scale, while the *flavon* controls hierarchies and mixings through powers of ϵ .

In 2HDM/MSSM (Type-II) realizations, one replaces $H \rightarrow (H_u, H_d)$ and $v \rightarrow (v_u, v_d)$ with $\tan\beta \equiv v_u/v_d$. In that case “factorize overall scales” means the fermion mass matrices pick up overall factors of v_u or v_d (depending on the sector), while the FN *exponents*, and hence the hierarchical structure, remain unchanged.

B. FN charges and exponents

The exponents n_{ij}^f are fixed by the $U(1)_{\text{FN}}$ charges of the fields, which we take from Ref. [3] as a simple viable assignment:

The FN exponents are obtained by demanding $U(1)_{\text{FN}}$ invariance of each operator, i.e.

¹ A numerical derivation of ϵ from m_e/m_τ is given in Sec. II C.

TABLE I. FN charges used in this work (quarks and two lepton options).

Sector	Field	Charges
Quarks	Q_i	(3, 2, 0)
	u_j^c	(4, 1, 0)
	d_j^c	(1, 0, 0)
Leptons (A)	L_i	(1, 0, 0)
	e_j^c	(4, 2, 0)
Leptons (B)	L_i	(0, 1, 0)
	e_j^c	(5, 1, 0)

- Up-type quarks: $\bar{Q}_i H u_j^c$ gives $n_{ij}^u = q(Q_i) + q(u_j^c)$,
- Down-type quarks: $\bar{Q}_i \tilde{H} d_j^c$ gives $n_{ij}^d = q(Q_i) + q(d_j^c)$,
- Charged leptons: $\bar{L}_i \tilde{H} e_j^c$ gives $n_{ij}^e = q(L_i) + q(e_j^c)$,
- Majorana neutrinos (Weinberg operator): $(L_i \tilde{H})(\bar{L}_j \tilde{H})$ gives $n_{ij}^v = q(L_i) + q(L_j)$.

For example, the (1, 1) entry of Y_u has exponent

$$n_{11}^u = q(Q_1) + q(u_1^c) = 3 + 4 = 7, \quad (4)$$

in agreement with Eq. (10) below.

For the quark and charged-lepton diagonal entries we will refer to the exponents

$$p_{u,c,t} = (7, 3, 0), \quad p_{d,s,b} = (4, 2, 0), \quad p_{e,\mu,\tau} = (5, 2, 0), \quad (5)$$

while for the mixing observables we take

$$p_{us} = 1, \quad p_{cb} = 2, \quad p_{ub} = 3, \quad p_{13} = 1, \quad (6)$$

so that $|V_{us}| \sim \epsilon$, $|V_{cb}| \sim \epsilon^2$, $|V_{ub}| \sim \epsilon^3$, and $\theta_{13}^{\text{PMNS}} \sim \epsilon$.

C. Determination of the hierarchical parameter ϵ

The hierarchical parameter $\epsilon \equiv 1/B$ is fixed by charged-lepton ratios, which we assume to scale as

$$m_e : m_\mu : m_\tau \propto \epsilon^5 : \epsilon^2 : 1. \quad (7)$$

The most robust ratio is m_e/m_τ , spanning the full charged-lepton hierarchy. Using RGE-run values at M_Z (approximately $m_e(M_Z) \approx 0.48$ MeV and $m_\tau(M_Z) \approx 1728$ MeV), we obtain

$$\frac{m_e(M_Z)}{m_\tau(M_Z)} \approx \frac{0.48 \text{ MeV}}{1728 \text{ MeV}} \approx 2.78 \times 10^{-4}. \quad (8)$$

Setting this equal to the model scaling ϵ^5 gives

$$\epsilon^5 \simeq 2.78 \times 10^{-4} \Rightarrow \epsilon \simeq (2.78 \times 10^{-4})^{1/5} \approx 0.194, \quad (9)$$

very close to the benchmark value $\epsilon = 0.187$ used throughout (corresponding to $B = 5.357$). The quoted value results from a more precise global fit across all observables, but is dominantly fixed by the charged-lepton hierarchy.

III. TEXTURES AND BENCHMARK COEFFICIENT MATRICES

A. FN textures

The quark Yukawa textures implied by the exponents discussed above can be written as

$$Y_u \sim C_u \circ \begin{pmatrix} \epsilon^7 & \epsilon^4 & \epsilon^3 \\ \epsilon^6 & \epsilon^3 & \epsilon^2 \\ \epsilon^4 & \epsilon^1 & 1 \end{pmatrix}, \quad (10)$$

$$Y_d \sim C_d \circ \begin{pmatrix} \epsilon^4 & \epsilon^3 & \epsilon^3 \\ \epsilon^3 & \epsilon^2 & \epsilon^2 \\ \epsilon^1 & 1 & 1 \end{pmatrix},$$

where “ \circ ” denotes the Hadamard (elementwise) product. The complex matrices $C_u = (C_{ij}^u)$ and $C_d = (C_{ij}^d)$ collect the residual $\mathcal{O}(1)$ coefficients, including CP phases; their magnitudes are expected to lie in an $\mathcal{O}(1)$ band (see Fig. 1 and Appendix A).

In the benchmark fit we work in a basis where the up Yukawa is diagonal, so all CKM mixing arises from Y_d . This choice is purely conventional; only the relative left-handed rotations of Y_u and Y_d are physical.

B. Extracted $\mathcal{O}(1)$ coefficients

To visualize the FN structure, we extract effective $\mathcal{O}(1)$ coefficients from observables by dividing out the predicted power of ϵ :

$$c_f \equiv \frac{y_f}{\epsilon^{p_f}}, \quad c_{V_{ij}} \equiv \frac{|V_{ij}|}{\epsilon^{p_{ij}}}, \quad c_{\theta_{13}} \equiv \frac{\theta_{13}^{\text{PMNS}}}{\epsilon^{p_{13}}}. \quad (11)$$

Here y_f are the Yukawa couplings obtained from quark and charged-lepton masses at M_Z , and we use the exponents p_f and p_{ij} defined above. For illustration we interpret the down-type Yukawas as Type-II 2HDM Yukawas with $\tan \beta = 40$, so that $y_{d,\ell} = m_{d,\ell}/v_d$ with $v_d \simeq v_{\text{SM}}/40$; the up-sector Yukawas use $v_u \simeq v_{\text{SM}}$. (The single-Higgs SM reinterpretation is discussed in Appendix A.)

C. Benchmark C matrices

To close the reproducibility gap we provide an explicit benchmark set of $\mathcal{O}(1)$ complex matrices C_u and C_d that, together with Eq. (10) at $\epsilon = 0.187$, exactly reproduce the target quark masses in Table II and the CKM magnitudes in Table III (up to trivial rephasings and rounding), when interpreted in a Type-II 2HDM with $\tan \beta = 40$.

We work in a basis where the up Yukawa matrix is diagonal, so that all CKM mixing arises from the down sector. In this basis one may take

$$Y_u = \text{diag}(y_u, y_c, y_t) = \text{diag}(m_u, m_c, m_t) \frac{\sqrt{2}}{v}, \quad (12)$$

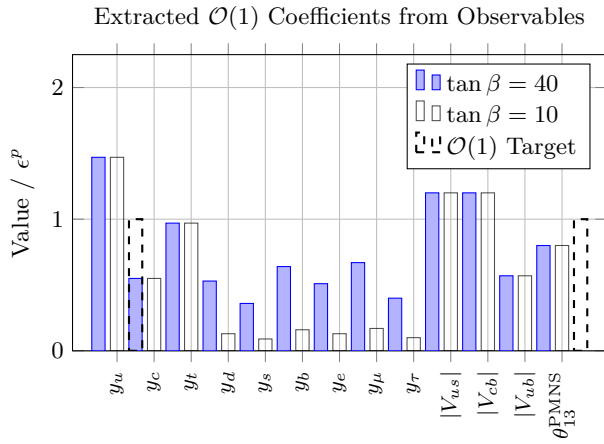


FIG. 1. Underlying $\mathcal{O}(1)$ coefficients, extracted by dividing observables by their predicted FN scaling power p . Masses are converted to Yukawas $y_f = m_f/v_f$ assuming a Type-II 2HDM, with $v_{\text{SM}} = 174.1$ GeV. Up-sector coefficients $\{y_u, y_c, y_t\}$ (using $v_u \approx v_{\text{SM}}$) and mixing coefficients $\{|V_{ij}|, \theta_{13}\}$ are independent of $\tan\beta$. Down-sector and lepton coefficients $\{y_d, y_s, y_b, y_e, y_\mu, y_\tau\}$ scale as $\approx \tan\beta$ (since $y_f = m_f/v_d$ and $v_d \simeq v_{\text{SM}}/\tan\beta$). The plot shows that $\tan\beta = 40$ keeps these coefficients $\mathcal{O}(1)$, while $\tan\beta = 10$ suppresses them to ~ 0.1 . Powers p are $\{y_u, y_c, y_t\} : \{7, 3, 0\}$, $\{y_d, y_s, y_b\} : \{4, 2, 0\}$, $\{y_e, y_\mu, y_\tau\} : \{5, 2, 0\}$, $\{|V_{us}|, |V_{cb}|, |V_{ub}|, \theta_{13}^{\text{PMNS}}\} : \{1, 2, 3, 1\}$. For the single-Higgs SM baseline, one instead takes $v_f = v_{\text{SM}}$ for all fermions; the down-sector and lepton coefficients are then uniformly reduced by a factor $\sim 1/40$, leaving the hierarchy of exponents unchanged (see Appendix A).

with $v = 174.1$ GeV, and enforce

$$Y_d = V_{\text{CKM}} \text{diag}(y_d, y_s, y_b), \quad (13)$$

where V_{CKM} is taken in the PDG parameterization with

$$|V_{us}| = 0.225, \quad |V_{cb}| = 0.0418, \quad |V_{ub}| = 0.00372, \quad \delta_{\text{CKM}} = 65.4^\circ.$$

The down Yukawas are interpreted as Type-II couplings, $y_{d,s,b} = m_{d,s,b}/v_d$ with $v_d \simeq v/\tan\beta$ and $\tan\beta = 40$.

The benchmark C matrices that implement this construction are:

$$C_u \approx \begin{pmatrix} 0.797 & 0 & 0 \\ 0 & 0.552 & 0 \\ 0 & 0 & 0.971 \end{pmatrix} \quad (14a)$$

and C_d =

$$\begin{pmatrix} 0.516 & 0.440 & 0.365 e^{-i1.14} \\ 0.0223 e^{+i\pi} & 0.356 & 0.768 \\ 2.97 \times 10^{-5} e^{-i0.395} & 5.26 \times 10^{-4} e^{+i\pi} & 0.642 \end{pmatrix} \quad (14b)$$

For completeness, we retain the illustrative neutrino-

sector coefficient matrix

$$K \approx \begin{pmatrix} 1.02 e^{+i0.40} & 0.97 e^{-i0.50} & 1.05 e^{+i0.90} \\ 0.97 e^{-i0.50} & 1.03 e^{+i0.20} & 0.99 e^{-i0.65} \\ 1.05 e^{+i0.90} & 0.99 e^{-i0.65} & 0.96 e^{+i0.10} \end{pmatrix}, \quad (14c)$$

which is used in the Majorana mass matrix M_ν below. All entries are quoted to three significant figures in magnitude (and in phase, where applicable). In particular, the diagonal elements of C_u are chosen such that

$$y_u = C_{u,11} \epsilon^7, \quad y_c = C_{u,22} \epsilon^3, \quad y_t = C_{u,33},$$

reproducing the up-type Yukawas from Table II. The down-sector matrix C_d is obtained by dividing the constructed Y_d by the FN powers in Eq. (10); its entries are all comfortably within the broad $\mathcal{O}(1)$ band.

D. Diagonalization and CKM power counting

Let U_L^f, U_R^f be the unitary matrices that diagonalize the Yukawas,

$$U_L^{f\dagger} Y_f U_R^f = \text{diag}(y_{f1}, y_{f2}, y_{f3}), \quad f = u, d. \quad (15)$$

The CKM matrix is $V_{\text{CKM}} = U_L^{u\dagger} U_L^d$.

Ignoring $\mathcal{O}(1)$ coefficients, the FN texture in Eq. (10) implies the scaling

$$U_L^u \sim \begin{pmatrix} 1 & \mathcal{O}(1) \epsilon & \mathcal{O}(1) \epsilon^3 \\ \mathcal{O}(1) \epsilon & 1 & \mathcal{O}(1) \epsilon^2 \\ \mathcal{O}(1) \epsilon^3 & \mathcal{O}(1) \epsilon^2 & 1 \end{pmatrix}, \quad (16a)$$

$$U_L^d \sim \begin{pmatrix} 1 & \mathcal{O}(1) \epsilon & \mathcal{O}(1) \epsilon^3 \\ \mathcal{O}(1) \epsilon & 1 & \mathcal{O}(1) \epsilon^2 \\ \mathcal{O}(1) \epsilon^3 & \mathcal{O}(1) \epsilon^2 & 1 \end{pmatrix}. \quad (16b)$$

Thus at leading order one finds

$$|V_{us}| \sim \epsilon, \quad |V_{cb}| \sim \epsilon^2, \quad |V_{ub}| \sim \epsilon^3, \quad (17)$$

which is borne out numerically by the benchmark fit.

For the explicit benchmark C matrices in Eq. (14), we find

$$U_L^u \approx \mathbb{I}, \quad (18a)$$

$$U_L^d \approx \begin{pmatrix} 0.974 & 0.225 & 0.00372 \\ -0.225 & 0.974 & 0.0418 \\ 0.00670 & -0.0414 & 0.999 \end{pmatrix}, \quad (18b)$$

to three significant figures. This realizes the standard picture where CKM mixing is dominantly sourced by the down sector. Right rotations are basis dependent and unobservable in charged currents; in the benchmark we take $U_R^u \approx \mathbb{I}$ and $U_R^d \approx \mathbb{I}$.

IV. LEPTON SECTOR AND PMNS

A. Neutrino sector and Takagi factorization

We assume neutrino masses are generated by the FN-suppressed Weinberg operator in Eq. (3). The resulting Majorana mass matrix can be written schematically as

$$M_\nu \sim K \circ \left(\epsilon^{n_{ij}^\nu} \right) \frac{v^2}{\Lambda_L}, \quad (19)$$

with K an $\mathcal{O}(1)$ complex symmetric matrix. For Majorana masses there is no independent U_R^ν ; instead a Takagi factorization diagonalizes M_ν :

$$U_\nu^T M_\nu U_\nu = \text{diag}(m_1, m_2, m_3), \quad m_i \geq 0. \quad (20)$$

The lepton mixing matrix is then

$$U_{\text{PMNS}} = U_e^\dagger U_\nu, \quad (21)$$

where U_e diagonalizes the charged-lepton Yukawa matrix Y_e (not shown explicitly).

For lepton option A in Table I, with L_i charges $(1, 0, 0)$, the neutrino exponents are

$$n_{ij}^\nu = q(L_i) + q(L_j) = \begin{pmatrix} 2 & 1 & 1 \\ 1 & 0 & 0 \\ 1 & 0 & 0 \end{pmatrix}, \quad (22)$$

so that

$$M_\nu \sim \frac{v^2}{\Lambda_L} K \circ \begin{pmatrix} \epsilon^2 & \epsilon & \epsilon \\ \epsilon & 1 & 1 \\ \epsilon & 1 & 1 \end{pmatrix}, \quad (23)$$

with each matrix element scaling as $\epsilon^{n_{ij}^\nu} = B^{-n_{ij}^\nu}$.

For the benchmark matrix K in Eq. (14c) and suitable charged-lepton rotations, we obtain the neutrino mixing moduli

$$|U_\nu| \approx \begin{pmatrix} 0.825 & 0.545 & 0.149 \\ 0.309 & 0.588 & 0.747 \\ 0.472 & 0.595 & 0.649 \end{pmatrix}, \quad (24)$$

corresponding to

$$(\theta_{12}, \theta_{23}, \theta_{13}) \simeq (33.4^\circ, 49.0^\circ, 8.60^\circ), \quad (25)$$

in good agreement with current global fits. The Dirac and Majorana phases do not affect these moduli.

B. Extraction of Dirac phases

For completeness we summarize how the Dirac CP phases are extracted from the benchmark mixing matrices.

CKM phase from V_{td} . We adopt the standard PDG parameterization of the CKM matrix with three angles $(\theta_{12}, \theta_{23}, \theta_{13})$ and one CP phase δ . At the precision relevant here we may take

$$s_{12} \equiv \sin \theta_{12} \simeq |V_{us}|, \quad s_{23} \simeq |V_{cb}|, \quad s_{13} \simeq |V_{ub}|,$$

and $c_{ij} \equiv \sqrt{1 - s_{ij}^2}$. In this parameterization the magnitude of V_{td} is

$$|V_{td}| = \left| s_{12}s_{23} - c_{12}c_{23}s_{13} e^{i\delta} \right|. \quad (26)$$

Squaring and solving for $\cos \delta$ gives

$$\cos \delta = \frac{(s_{12}s_{23})^2 + (c_{12}c_{23}s_{13})^2 - |V_{td}|^2}{2 s_{12}s_{23} c_{12}c_{23} s_{13}}. \quad (27)$$

Using the benchmark values $s_{12} = 0.225$, $s_{23} = 0.0418$, $s_{13} = 0.00372$, and $|V_{td}| = 0.00856$ yields

$$|V_{td}| \simeq 0.00856, \quad \delta_{\text{CKM}} \simeq 65.4^\circ. \quad (28)$$

PMNS phase from unitarity. For the leptons we adopt the PDG parameterization of U_{PMNS} with three angles $(\theta_{12}, \theta_{23}, \theta_{13})$ and a Dirac phase δ_{PMNS} . Defining $s_{ij} \equiv \sin \theta_{ij}$, $c_{ij} \equiv \cos \theta_{ij}$, the elements $U_{\mu 1}$ and $U_{\tau 1}$ take the form

$$U_{\mu 1} = -s_{12}c_{23} - c_{12}s_{23}s_{13} e^{i\delta_{\text{PMNS}}}, \quad (29)$$

$$U_{\tau 1} = s_{12}s_{23} - c_{12}c_{23}s_{13} e^{i\delta_{\text{PMNS}}}. \quad (30)$$

Taking magnitudes squared yields relations for $\cos \delta_{\text{PMNS}}$,

$$\cos \delta_{\text{PMNS}} = \frac{|U_{\mu 1}|^2 - s_{12}^2 c_{23}^2 - c_{12}^2 s_{23}^2 s_{13}^2}{2 s_{12} c_{12} c_{23} s_{23} s_{13}}, \quad (31)$$

or equivalently

$$\cos \delta_{\text{PMNS}} = \frac{s_{12}^2 s_{23}^2 + c_{12}^2 c_{23}^2 s_{13}^2 - |U_{\tau 1}|^2}{2 s_{12} c_{12} c_{23} s_{23} s_{13}}. \quad (32)$$

Using the benchmark angles $\theta_{12} = 33.4^\circ$, $\theta_{23} = 49.0^\circ$, $\theta_{13} = 8.60^\circ$ and the moduli $|U_{\mu 1}| = 0.309$, $|U_{\tau 1}| = 0.472$ from Eq. (24), one finds

$$\delta_{\text{PMNS}} \simeq 230^\circ, \quad (33)$$

up to the usual ambiguity from $\cos \delta$.

V. NUMERICAL RESULTS

A. Quark masses and CKM matrix

The benchmark C matrices in Eq. (14), together with $\epsilon = 0.187$ and a Type-II 2HDM interpretation with $\tan \beta = 40$, reproduce the quark masses shown in Table II. The light-quark masses at M_Z are obtained by

TABLE II. Quark masses at M_Z (3 s.f.). “PDG $\rightarrow M_Z$ ” indicates RGE running from PDG reference scales [5]; quoted light-quark errors include small theory pads for running and matching.

Observable	PDG $\rightarrow M_Z$	Model
m_u [MeV]	1.29 ± 0.20	1.11
m_d [MeV]	2.80 ± 0.20	2.82
m_s [MeV]	55.7 ± 1.3	55.7
m_c [GeV]	0.629 ± 0.012	0.629
m_b [GeV]	2.794 ± 0.034	2.794
m_t [GeV]	169 ± 1.1	169

TABLE III. CKM magnitudes at M_Z [5]. Running to M_Z is negligible at this precision.

Observable	PDG ref.	Model
$ V_{us} $	0.22501 ± 0.00068	0.225
$ V_{cb} $	$0.0418^{+0.0008}_{-0.0007}$	0.0418
$ V_{ub} $	$0.003732^{+0.000090}_{-0.000085}$	0.00372

running PDG reference-scale values [5]; small theory errors from running and matching are included.

The CKM magnitudes at M_Z are summarized in Table III; running effects on the CKM elements are negligible at the quoted precision.

The full CKM matrix (moduli) obtained from $U_L^{u\dagger} U_L^d$ is

$$V_{CKM} \approx \begin{pmatrix} 0.974 & 0.225 & 0.00373 \\ 0.2249 & 0.973 & 0.0418 \\ 0.00856 & 0.0411 & 0.999 \end{pmatrix}, \quad (34)$$

while the phase structure, in a convenient convention, can be summarized as

$$\arg V_{CKM} [\text{deg}] \approx \begin{pmatrix} 0 & 0 & -65.4 \\ +180 & 0 & 0 \\ -22.7 & +179 & 0 \end{pmatrix}. \quad (35)$$

B. Neutrino mixing and PMNS matrix

The benchmark neutrino-sector fit (using K from Eq. (14c) in texture A) yields the PMNS matrix

$$U_{\text{PMNS}} \approx \begin{pmatrix} 0.825 & 0.545 & 0.149 \\ 0.309 & 0.588 & 0.747 \\ 0.472 & 0.595 & 0.649 \end{pmatrix}, \quad (36)$$

corresponding to the mixing angles in Eq. (24). A convenient phase convention is

$$\arg U_{\text{PMNS}} [\text{deg}] \approx \begin{pmatrix} 0 & 0 & -230 \\ -13.4 & +4.6 & 0 \\ +7.6 & -4.0 & 0 \end{pmatrix}. \quad (37)$$

The overall right Majorana phase factor $\text{diag}(1, e^{i\alpha_{21}/2}, e^{i\alpha_{31}/2})$ is omitted in Eq. (36) to save space; it is understood in derived quantities such as $m_{\beta\beta}$.

C. Neutrino mass spectrum, $\sum m_\nu$, and $m_{\beta\beta}$

Oscillation experiments determine the mass-squared splittings $\Delta m_{21}^2 \equiv m_2^2 - m_1^2$ and $\Delta m_{31}^2 \equiv m_3^2 - m_1^2$, but not the absolute scale or ordering. Current global fits favor the normal ordering (NO) with $\Delta m_{21}^2 \simeq 7.4 \times 10^{-5} \text{ eV}^2$ and $|\Delta m_{31}^2| \simeq 2.5 \times 10^{-3} \text{ eV}^2$ [5].

For the benchmark FN texture and the mixing matrix in Eq. (24), we adopt a representative NO spectrum with lightest mass

$$m_1 \simeq 4.0 \text{ meV}, \quad (38)$$

which then fixes

$$m_2 \simeq 9.6 \text{ meV}, \quad m_3 \simeq 50 \text{ meV}, \quad (39)$$

corresponding to

$$\Delta m_{21}^2 \simeq 7.6 \times 10^{-5} \text{ eV}^2, \quad \Delta m_{31}^2 \simeq 2.5 \times 10^{-3} \text{ eV}^2, \quad (40)$$

in good agreement with oscillation data [5]. The sum of neutrino masses is then

$$\sum m_\nu \equiv m_1 + m_2 + m_3 \simeq 0.064 \text{ eV}, \quad (41)$$

just above the minimal value allowed by NO and comfortably below current cosmological upper bounds $\sum m_\nu \lesssim 0.1 \text{ eV}$ within ΛCDM [5].

Neutrino masses as powers of B . For lepton option A in Table I, the FN charges fix the neutrino exponents to $n_{ij}^\nu = q(L_i) + q(L_j) = \begin{pmatrix} 2 & 1 & 1 \\ 1 & 0 & 0 \\ 1 & 0 & 0 \end{pmatrix}$, so that $(M_\nu)_{ij} \propto \epsilon^{n_{ij}^\nu} = B^{-n_{ij}^\nu}$. Diagonalizing the benchmark texture one finds that the three Majorana eigenvalues are very well described by

$$(m_1, m_2, m_3) \simeq (2.3 B^{-2}, 1.0 B^{-1}, 1.0) \frac{v^2}{\Lambda_L}, \quad (42)$$

i.e. effective FN powers $(n_1, n_2, n_3) \simeq (2, 1, 0)$ with $\mathcal{O}(1)$ prefactors. For the benchmark value $B = 5.357$ ($\epsilon = 1/B \simeq 0.187$) and $v^2/\Lambda_L \simeq 50 \text{ meV}$ ($\Lambda_L \simeq 6 \times 10^{14} \text{ GeV}$), Eq. (42) gives

$$(m_1, m_2, m_3) \simeq (4.0, 9.6, 50) \text{ meV}, \quad (43)$$

corresponding to $\Delta m_{21}^2 \simeq 7.6 \times 10^{-5} \text{ eV}^2$, $\Delta m_{31}^2 \simeq 2.5 \times 10^{-3} \text{ eV}^2$ and $\sum m_\nu \simeq 0.064 \text{ eV}$ in normal ordering. Thus, once B is fixed by the charged-lepton hierarchy, the pattern of neutrino masses follows directly from their FN powers, while the overall scale is controlled by the single additional parameter Λ_L .

The effective Majorana mass probed by neutrinoless double beta decay is

$$m_{\beta\beta} \equiv \left| \sum_{i=1}^3 U_{ei}^2 m_i e^{i\alpha_i} \right|, \quad (44)$$

where U_{ei} are the elements of the first row of U_{PMNS} and α_i are the (unknown) Majorana phases. Using the benchmark mixing moduli $|U_{e1}| = 0.825$, $|U_{e2}| = 0.545$, $|U_{e3}| = 0.149$ and the mass spectrum above, we find that $m_{\beta\beta}$ lies in the band

$$m_{\beta\beta} \simeq (0\text{--}7) \text{ meV}, \quad (45)$$

where the lower edge corresponds to finely tuned destructive interference among the three terms. For generic $\mathcal{O}(1)$ Majorana phases one expects $m_{\beta\beta}$ of order a few meV.

This is well below present experimental limits, which translate to $m_{\beta\beta} \lesssim (30\text{--}150)$ meV once nuclear-matrix-element uncertainties are included [5], but it lies in the target range of future ton-scale searches (such as LEGEND-1000 and nEXO). In this sense the one-flavon FN framework provides concrete, testable benchmarks for both the cosmological observable $\sum m_\nu$ and the laboratory observable $m_{\beta\beta}$.

D. CP violation

The benchmark fit predicts both quark and lepton Dirac CP phases. Inserting the benchmark angles and $\delta_{\text{CKM}} \simeq 65.4^\circ$ into the standard expression for the Jarlskog invariant [6],

skog invariant [6],

$$J_{\text{CKM}} = s_{12} s_{23} s_{13} c_{12} c_{23} c_{13}^2 \sin \delta_{\text{CKM}} \simeq 3.11 \times 10^{-5}, \quad (46)$$

we obtain excellent agreement with the PDG average [5], $J_{\text{CKM}} = (3.08^{+0.15}_{-0.13}) \times 10^{-5}$.

For the lepton sector, the benchmark fit yields a Dirac phase $\delta_{\text{PMNS}} \simeq 230^\circ$, with associated Jarlskog invariant

$$J_{\text{PMNS}} = s_{12} s_{23} s_{13} c_{12} c_{23} c_{13}^2 \sin \delta_{\text{PMNS}} \simeq -2.55 \times 10^{-2}, \quad (47)$$

notably much larger in magnitude than in the quark sector. Upcoming measurements of leptonic CP violation thus provide an incisive probe of the FN charge assignments.

VI. SIGNIFICANCE AND OUTLOOK

A *single hierarchical* parameter B —fixed by charged-lepton ratios—organizes quark and lepton hierarchies with near-unity coefficients, reproducing masses and leading CKM/PMNS patterns at M_Z in a one-flavon FN framework. Simple power counting in $\epsilon = 1/B$ yields $|V_{us}| \sim \epsilon$, $|V_{cb}| \sim \epsilon^2$, $|V_{ub}| \sim \epsilon^3$, and $\theta_{13}^{\text{PMNS}} \sim \epsilon$, as visualized in Fig. 1. The model provides concrete targets for the neutrino sector, with a normal ordering, $\sum m_\nu \simeq 0.064$ eV, and $m_{\beta\beta}$ in the few-meV range, together with a realistic U_{PMNS} .

Crucially, the framework *also* predicts CP violation: the benchmark fit fixes $\delta_{\text{CKM}} \simeq 65.4^\circ$ with $J_{\text{CKM}} \simeq 3.1 \times 10^{-5}$ (Eq. (46)) and $\delta_{\text{PMNS}} \simeq 230^\circ$ (Eq. (47)). Future precision in lepton mixing moduli, direct and cosmological probes of $\sum m_\nu$, and $m_{\beta\beta}$ bands can serve as discriminants among FN charge choices and may point toward a more complete theory of flavor.

[1] C. D. Froggatt and H. B. Nielsen, Hierarchy of Quark Masses, Cabibbo Angles and CP Violation, *Nucl. Phys. B* **147**, 277 (1979).

[2] M. Leurer, Y. Nir, and N. Seiberg, “Mass matrix models,” *Nucl. Phys. B* **398**, 319 (1993), doi:10.1016/0550-3213(93)90072-P, arXiv:hep-ph/9212278.

[3] C. Cornella, D. Curtin, E. T. Neil, and J. O. Thompson, Mapping and probing Froggatt–Nielsen solutions to the quark flavor puzzle, *Phys. Rev. D* **111**, 015042 (2025), doi:10.1103/PhysRevD.111.015042, arXiv:2306.08026.

[4] S. Weinberg, “Baryon- and Lepton-Nonconserving Processes,” *Phys. Rev. Lett.* **43**, 1566 (1979), doi:10.1103/PhysRevLett.43.1566.

[5] Particle Data Group, Review of Particle Physics, *Phys. Rev. D* **110**, 030001 (2024).

[6] C. Jarlskog, Commutator of the Quark Mass Matrices in the Standard Electroweak Model and a Measure of Maximal CP Nonconservation, *Phys. Rev. Lett.* **55**, 1039 (1985).

Appendix A: FN coefficients: Type-II 2HDM vs single-Higgs SM

In the main text we emphasized that the *hierarchy* is carried by powers of ϵ in Eq. (10), while the residual coefficients are $\mathcal{O}(1)$. Here we make this statement more explicit by extracting the FN coefficients from observables and comparing

two interpretations:

1. a Type-II 2HDM/MSSM-like setting with $\tan \beta = 40$, and
2. the single-Higgs Standard Model with $v_{\text{SM}} = 174.1$ GeV.

Throughout we use the exponents already fixed by Eq. (10):

$$p_{u,c,t} = (7, 3, 0), \quad p_{d,s,b} = (4, 2, 0), \quad p_{e,\mu,\tau} = (5, 2, 0),$$

and, for mixings,

$$p_{us} = 1, \quad p_{cb} = 2, \quad p_{ub} = 3, \quad p_{13} = 1.$$

1. Definition of FN coefficients

For any fermion f with FN exponent p_f we define the dimensionless FN coefficient

$$c_f \equiv \frac{y_f}{\epsilon^{p_f}}, \quad (\text{A1})$$

where y_f is the corresponding Yukawa coupling and $\epsilon = 1/B = 1/5.357 \simeq 0.187$. For mixing observables,

$$c_{V_{ij}} \equiv \frac{|V_{ij}|}{\epsilon^{p_{ij}}}, \quad c_{\theta_{13}} \equiv \frac{\theta_{13}^{\text{PMNS}}}{\epsilon^{p_{13}}}. \quad (\text{A2})$$

A successful FN model should yield c coefficients that are broadly $\mathcal{O}(1)$.

2. Type-II 2HDM interpretation ($\tan \beta = 40$)

In a Type-II 2HDM, up-type fermions couple to H_u and down-type fermions and charged leptons couple to H_d . Writing

$$v_{\text{SM}} = 174.1 \text{ GeV}, \quad \tan \beta = \frac{v_u}{v_d}, \quad (\text{A3})$$

we have

$$v_u = v_{\text{SM}} \sin \beta, \quad v_d = v_{\text{SM}} \cos \beta. \quad (\text{A4})$$

For $\tan \beta = 40$, $v_u \simeq v_{\text{SM}}$ and $v_d \simeq v_{\text{SM}}/40$. The Yukawa couplings are

$$y_{u_i} = \frac{m_{u_i}}{v_u}, \quad y_{d_i} = \frac{m_{d_i}}{v_d}, \quad y_{\ell_i} = \frac{m_{\ell_i}}{v_d}. \quad (\text{A5})$$

Using the quark and charged-lepton masses at M_Z and the FN powers specified above, the up-sector and mixing coefficients are (as in Fig. 1)

$$c_{y_u} \approx 1.47, \quad c_{y_c} \approx 0.55, \quad c_{y_t} \approx 0.97, \quad (\text{A6})$$

$$c_{V_{us}} \approx 1.20, \quad c_{V_{cb}} \approx 1.20, \quad c_{V_{ub}} \approx 0.57, \quad c_{\theta_{13}} \approx 0.80. \quad (\text{A7})$$

For down-type quarks and charged leptons one finds

$$c_{y_d}^{(2\text{HDM})} \approx 0.53, \quad c_{y_s}^{(2\text{HDM})} \approx 0.36, \quad c_{y_b}^{(2\text{HDM})} \approx 0.64, \quad (\text{A8})$$

$$c_{y_e}^{(2\text{HDM})} \approx 0.51, \quad c_{y_\mu}^{(2\text{HDM})} \approx 0.67, \quad c_{y_\tau}^{(2\text{HDM})} \approx 0.40. \quad (\text{A9})$$

All of these lie in a comfortable $\mathcal{O}(1)$ band ($\sim 0.4\text{--}1.5$), motivating the choice of relatively large $\tan \beta$ in this framework.

TABLE A1. FN coefficients $c_f \equiv y_f/\epsilon^{p_f}$ for down-type quarks and charged leptons, comparing a Type-II 2HDM interpretation with $\tan \beta = 40$ to the single-Higgs SM interpretation. The FN exponents are $p_{d,s,b} = \{4, 2, 0\}$ and $p_{e,\mu,\tau} = \{5, 2, 0\}$.

Observable	p_f	$c_f^{(2\text{HDM})}$ ($\tan \beta = 40$)	$c_f^{(\text{SM})}$ (one Higgs)
y_d	4	0.53	1.3×10^{-2}
y_s	2	0.36	9.0×10^{-3}
y_b	0	0.64	1.6×10^{-2}
y_e	5	0.51	1.3×10^{-2}
y_μ	2	0.67	1.7×10^{-2}
y_τ	0	0.40	1.0×10^{-2}

3. Single-Higgs SM interpretation

In the single-Higgs SM, all fermions couple to the same Higgs doublet with vev v_{SM} , so

$$y_f^{(\text{SM})} = \frac{m_f}{v_{\text{SM}}} \quad (\text{A10})$$

for every quark or charged lepton. The up-sector and mixing coefficients remain exactly the same as above, since we already used $v_u \simeq v_{\text{SM}}$ for those sectors. For down-type quarks and charged leptons, however, the coefficients are reduced relative to the $\tan \beta = 40$ Type-II interpretation,

$$c_f^{(\text{SM})} = \frac{m_f}{v_{\text{SM}} \epsilon^{p_f}} = \frac{v_d}{v_{\text{SM}}} \frac{m_f}{v_d \epsilon^{p_f}} \simeq \frac{1}{40} c_f^{(2\text{HDM})}, \quad (\text{A11})$$

so numerically

$$c_{y_d}^{(\text{SM})} \approx 1.3 \times 10^{-2}, \quad c_{y_s}^{(\text{SM})} \approx 9.0 \times 10^{-3}, \quad c_{y_b}^{(\text{SM})} \approx 1.6 \times 10^{-2}, \quad (\text{A12})$$

$$c_{y_e}^{(\text{SM})} \approx 1.3 \times 10^{-2}, \quad c_{y_\mu}^{(\text{SM})} \approx 1.7 \times 10^{-2}, \quad c_{y_\tau}^{(\text{SM})} \approx 1.0 \times 10^{-2}. \quad (\text{A13})$$

These are still technically “order one” in a very broad sense, but cluster around 10^{-2} rather than around unity. The Type-II 2HDM with large $\tan \beta$ can therefore be viewed as a reparametrization that lifts these coefficients into a more aesthetically pleasing $\mathcal{O}(1)$ band without changing the underlying FN exponents.

4. Comparison table

For quick reference, Table A1 shows the FN coefficients for the down-type quarks and charged leptons in the $\tan \beta = 40$ Type-II 2HDM interpretation and in the single-Higgs SM interpretation side by side.